Spin Stripe Order in a Square Planar Trilayer Nickelate

Junjie Zhang,[1,2] D. M. Pajerowski,[3] A. S. Botana,[1,4] Hong Zheng,[1] L. Harriger,[5] J. Rodriguez-Rivera,[5,6] J. P. C. Ruff,[7] N. J. Schreiber,[8] B. Wang,[1] Yu-Sheng Chen,[9] W. C. Chen,[5,6] M. R. Norman,[1] S. Rosenkranz,[1] J. F. Mitchell,[1] and D. Phelan[1]

[1]*Materials Science Division, Argonne National Laboratory, Argonne, Illinois 60439, USA*
[2]*Materials Science and Technology Division, Oak Ridge National Laboratory, Oak Ridge, Tennessee 37831, USA*
[3]*Neutron Scattering Division, Oak Ridge National Laboratory, Oak Ridge, Tennessee 37831, USA*
[4]*Department of Physics, Arizona State University, Tempe, Arizona 85287, USA*
[5]*NIST Center for Neutron Research, National Institute of Standards and Technology, Gaithersburg, Maryland 20899, USA*
[6]*Department of Materials Sciences, University of Maryland, College Park, Maryland 20742, USA*
[7]*CHESS, Cornell University, Ithaca, New York 14853, USA*
[8]*Department of Materials Science and Engineering, Cornell University, Ithaca, New York 14853, USA*
[9]*ChemMatCARS, The University of Chicago, Argonne, Illinois 60439, USA*

(Received 9 January 2018; revised manuscript received 14 March 2019; published 18 June 2019)

Trilayer nickelates, which exhibit a high degree of orbital polarization combined with an electron count ($d^{8.67}$) corresponding to overdoped cuprates, have been identified as a promising candidate platform for achieving high-T_c superconductivity. One such material, $La_4Ni_3O_8$, undergoes a semiconductor-insulator transition at ~105 K, which was recently shown to arise from the formation of charge stripes. However, an outstanding issue has been the origin of an anomaly in the magnetic susceptibility at the transition and whether it signifies the formation of spin stripes akin to single layer nickelates. Here we report single crystal neutron diffraction measurements (both polarized and unpolarized) that establish that the ground state is indeed magnetic. The ordering is modeled as antiferromagnetic spin stripes that are commensurate with the charge stripes, the magnetic ordering occurring in individual trilayers that are essentially uncorrelated along the crystallographic c axis. A comparison of the charge and spin stripe order parameters reveals that, in contrast to single-layer nickelates such as $La_{2-x}Sr_xNiO_4$ as well as related quasi-2D oxides including manganites, cobaltates, and cuprates, these orders uniquely appear simultaneously, thus demonstrating a stronger coupling between spin and charge than in these related low-dimensional correlated oxides.

DOI: 10.1103/PhysRevLett.122.247201

There has been intense interest in stripe phases due to the interplay of charge, spin, and lattice degrees of freedom as well as their relevance to high-temperature superconductivity in cuprates [1–9]. Uncovering cupratelike superconductivity in oxides containing transition metals other than copper remains a daunting challenge [10], and in this regard $R_4Ni_3O_8$ (R = La, Pr, or Nd) compounds have emerged as potential candidates [11–13]. These layered materials possess structures that resemble the $n = 3$ Ruddlesden-Popper phase ($R_{n+1}Ni_nO_{3n+1}$) [14], but they differ in that all apical oxygens are absent, resulting in trilayers of NiO_2 planes in which all Ni ions possess square-planar coordination of oxygen anions. The electron count ($3d^{8.67}$) coincides with the overdoped regime of cuprates [12,15]. Recent work indicates that these nickelates possess a low-spin state of Ni, large orbital polarization of the e_g states with predominantly $d_{x^2-y^2}$ orbital character near the Fermi energy, and significant O $2p$ – Ni $3d$ hybridization, all of which are considered to be important ingredients for superconductivity in the high-T_c cuprates [12]. Thus $R_4Ni_3O_8$ compounds (particularly $Pr_4Ni_3O_8$ which is metallic [12]) are more similar to the superconducting cuprates than previously studied nickelates with octahedral coordination, such as $La_{2-x}Sr_xNiO_4$ (LSNO) [16–18] and $LaNiO_3$-based heterostructures [19].

Unlike metallic $Pr_4Ni_3O_8$, $La_4Ni_3O_8$ undergoes a semiconductor-insulator transition upon cooling through ~105 K [11,13,20–28], and we have recently shown that the insulating state possesses charge stripes [13]. Stripes form in the Ni-O planes and are oriented at 45° to the Ni-O bonds, tripling the unit cell along the propagation direction. This tripling can be modeled as an ordering of charges in a 2:1 ratio [consistent with a splitting of the nominal charge concentration ($Ni^{4/3+}$) into Ni^{1+} and Ni^{2+} ions], and the ensuing threefold superlattice that forms is similar to that found in single-layer LSNO ($x = 1/3$) [29]. Unanswered, however, is whether the ground state is magnetically ordered. Magnetic ordering has not been detected by neutron powder diffraction [11]. However, ^{139}La nuclear magnetic resonance measurements have revealed dramatic spectral changes attributed to low-energy antiferromagnetic correlations [20] and argued to be associated with the onset of long-range magnetic order below 105 K. Recent density functional theory (DFT) calculations were consistent with a

commensurate charge and spin-stripe ordered ground state [27]. Here, we report evidence from single crystal neutron diffraction measurements that the Ni-O trilayers are magnetically ordered due to the formation of antiferromagnetic spin stripes. The neutron intensity can be modeled with *ab*-plane spin stripes formed within trilayer blocks, with the blocks uncorrelated along the *c* axis. These spin stripes are commensurate with the charge stripes, and both form simultaneously at the semiconductor-insulator transition below ~105 K, a distinct contrast to charge and spin stripe ordering in LSNO, other quasi-2D oxides, and the vast majority of transition metal oxides.

Neutron diffraction was performed on a single crystal (~50 mg) obtained via reduction of a Ruddlesden-Popper $La_4Ni_3O_{10}$ crystal grown by the floating-zone method under high-pO_2 [13]. The reduction left the crystal brittle with a large, structured mosaic (~7° at full-width-half-maximum). The crystal was encapsulated in Cytop CTL-809M [30], an amorphous fluorinated epoxy that is commonly employed to avoid the incoherent background from hydrogen-containing epoxies. Nevertheless, $|\vec{Q}|$-dependent backgrounds were observed, likely arising from quasi-elastic scattering from the epoxy, and we have therefore subtracted backgrounds measured above 105 K to reveal the intrinsic signal from the crystal in unpolarized measurements. Unpolarized measurements in the (*hk*0) scattering plane were performed on the MACS cold neutron triple axis spectrometer at the NIST Center for Neutron Research (NCNR) with $\lambda = 4.05$ Å. Polarized measurements in the (*h*0*l*) plane were performed on MACS using ^{3}He polarizers [31–33] with the neutron spin polarization oriented out of the plane (along the [010]) direction with fixed $E_i = E_f = 5.0$ meV. For the polarized measurements, MACS was operated in single-detector triple-axis mode. Polarization efficiency corrections were made to the MACS data shown in the Letter; uncorrected scans are shown in the Supplemental Material [34]. Unpolarized measurements in the (*h*0*l*) scattering plane were performed on the triple-axis HB-1A at HFIR with $\lambda = 2.37$ Å with collimations of 48'−40'−40'−120'. High-resolution single crystal x-ray diffraction experiments were performed on a 0.6 mg single crystal in a displex at beamline A2 at the Cornell High Energy Synchrotron Source (CHESS) ($\lambda = 0.363803$ Å). We employ pseudotetragonal notation (space group $F4/mmm$) with lattice constants of $a = b \sim 5.6$ and $c \sim 26.1$ Å for which the $\vec{a}$ and $\vec{b}$ axes are oriented 45° to the Ni-O bonds and correspond to the propagation directions of the charge stripes [13] (see the Supplemental Material [34], Fig. S1 for a diagram that relates these two cells).

The unpolarized reciprocal space map of the (*hk*0) scattering plane obtained at base temperature (1.8 K) with 120 K data subtracted as a background is shown in Fig. 1(a). Weak peaks are observed at (2/3, 0, 0), (4/3, 0, 0),

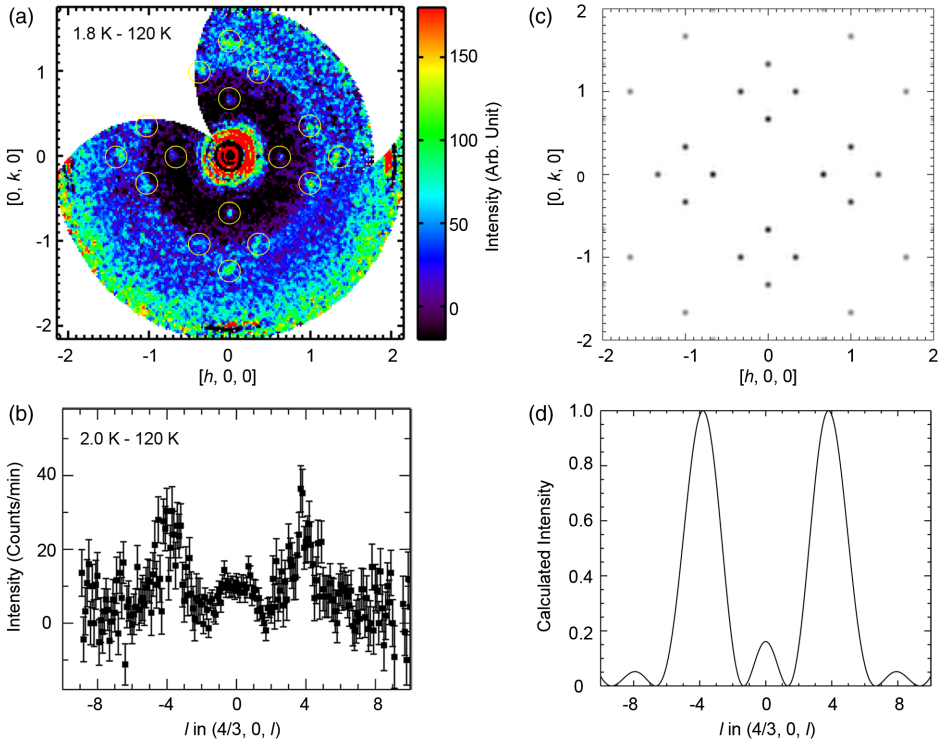

FIG. 1. (a) Unpolarized neutron scattering intensity in the (*hk*0) plane measured for $La_4Ni_3O_8$ at $T = 1.8$ K with 120 K data subtracted. (b) Scan along $(4/3, 0, l)$ at $T = 2.0$ K with 120 K data subtracted. Uncertainties represent one standard deviation, derived from the square roots of the numbers of counts. The simulated intensities in the (*hk*0) plane as well as along $(4/3, 0, l)$ for the uncorrelated trilayer model described in the text and shown in Fig. 3 are shown in (c) and (d), respectively.

(1, 1/3, 0), and symmetrically equivalent positions. These peaks occur at the same points reported in single-crystal x-ray diffraction and correspond to the positions assigned to charge stripes [13]. Since the charge peaks are sharp in h and k in x-ray diffraction [13], there is not contamination from a diffuse nuclear component in this plane. Since neutrons are not directly sensitive to modulations in charge, the results imply one of three possibilities: (i) the scattering is of nuclear origin arising from atomic displacements that follow the charge stripe modulation; (ii) the scattering is magnetic, such as from spin stripes; or (iii) both (i) and (ii). In single layer (e.g., LSNO, $x \leq 0.5$) nickelates [7], $\vec{q}_s = 1/2\vec{q}_c$, where $\vec{q}_s$ and $\vec{q}_c$ are the spin-stripe and charge-stripe wave vectors, respectively. $\vec{q}_c$ is measured from the Γ point, whereas $\vec{q}_s$ is measured from the antiferromagnetic wave vector [e.g., 100, which corresponds to the (π,π) point in the $I4/mmm$ setting with $a = b \sim 3.9$ Å]. Thus, when $\vec{q}_c = (2/3, 0, 0)$, then $\vec{q}_s = (1/3, 0, 0)$ and the charge and spin-stripe reflections ($\vec{\tau}_c$ and $\vec{\tau}_s$) coincide, e.g., at $\vec{\tau}_c = (0, 0, 0) + (2/3, 0, 0)$ and $\vec{\tau}_s = (1, 0, 0) - (1/3, 0, 0)$, making scenarios (i), (ii), and (iii) all possible.

To distinguish among these three possibilities, we measured the l dependence of the neutron peaks. Figure 1(b) shows an unpolarized scan along $(4/3, 0, l)$. A weak, broad peak is observed that is centered at $l = 0$, and stronger broad peaks are present at $l = \pm 4$. This differs from the x-ray measurements, in which pseudotriplets centered at $l = 8n$ (e.g., $l = -1, 0, 1$ and $l = 7, 8, 9$) occur because the repeat distance for charge along $\vec{c}$ is the nearest distance between Ni-O planes, which is $c/8$ [13]. The difference in l dependence arises from the magnetic contribution to the neutron cross section, and the fact that the peaks are centered at $l = 4n$ establishes a nearest-neighbor antiferromagnetic interaction along $\vec{c}$ so that the repeat distance is twice that between nearest-neighboring Ni-O planes, i.e., $c/4$. This realization, combined with the broad nature of the peaks, suggestive of short-range correlations, led us to consider magnetic correlations within individual, uncorrelated trilayers.

To further establish the magnetic ordering, we performed neutron polarization analysis. All coherent nuclear scattering is non-spin flip (NSF). On MACS, where neutron polarization is vertically out of the scattering plane (along $\vec{b}$), the component of spin that is parallel to $\vec{b}$ will give rise to a NSF magnetic cross section, whereas the component of spin that is both in the $h0l$ plane and perpendicular to (4/3,0,4), i.e., along $-0.54\hat{a} + 0.84\hat{c}$, gives rise to a spin-flip (SF) cross section. Figures 2(a) (SF) and 2(b) (NSF) show scans at 1.5 and 120 K through (4/3, 0, 4), which is a position that we identified as magnetic above based on the fact that it appears at $l = 4$. A peak is clearly visible at 1.5 K in the SF channel, but not in the NSF channel, nor in either channel at 120 K. This then confirms the magnetic origin of (4/3, 0, 4), and indicates that the ordered moment possesses a significant component along $-0.54\hat{a} + 0.84\hat{c}$,

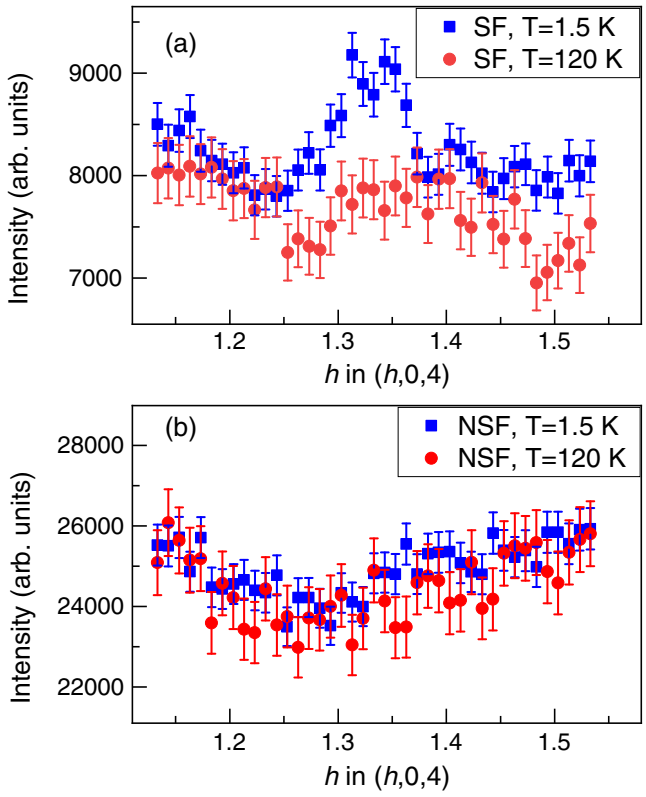

FIG. 2. Spin polarized neutron diffraction from $La_4Ni_3O_8$ as measured on MACS in the ($h0l$) plane with neutron spin polarization perpendicular to the plane. (a) Scans along (h, 0, 0) through (4/3,0,4) in the spin-flip channel at 1.5 (blue) and 120 K (red). (b) The same scans in the non-spin-flip channel. Uncertainties represent one standard deviation, derived from the square roots of the number of counts. Data have been corrected for polarization efficiency.

but lacks a significant component along $\vec{b}$. We performed additional polarized measurements on the (4/3,0,0) peak, and the measurements were consistent with contributions from both nuclear and magnetic order (See the Supplemental Material [34]), the SF cross section being sensitive to the component of spin in the $\hat{b} - \hat{c}$ plane. Combined, the polarization measurements are consistent with ordered spins that point along $\vec{c}$.

By analogy with the single layer nickelates, $\vec{q}_s = \frac{1}{2}\vec{q}_c$ implies the formation of antiferromagnetic spin stripes in the NiO_2 planes, commensurate with the charge. Using the charge stripe structure [13] as a starting point (Fig. 3), models of antiferromagnetic stripes within each individual layer of a trilayer were constructed. Consistent with DFT calculations as well as x-ray absorption spectroscopy [12], the models have finite $S = 1/2$ spins only on Ni^{1+}, whereas Ni^{2+} (being in a low spin state) have no moment. Following expectations for 180° superexchange on a square planar lattice, we have taken the nearest-neighbor Ni^{1+}-Ni^{1+} interactions to be antiferromagnetic. Under these constraints, models for uncorrelated trilayers possess

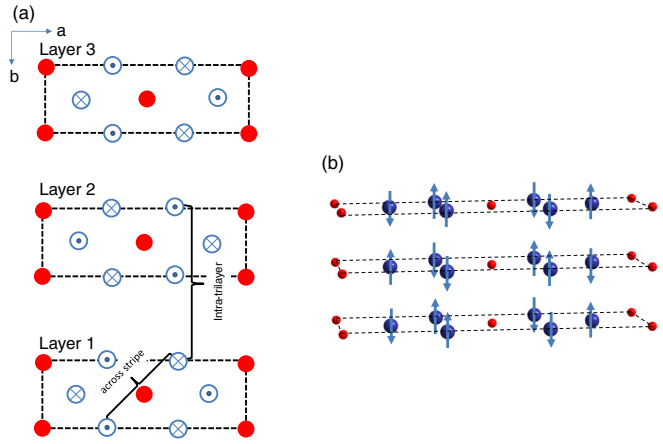

FIG. 3. (a) Uncorrelated trilayer model for the spin ordering, displayed layer by layer. Ni^{1+} sites are shown in blue, and nonmagnetic Ni^{2+} sites are shown in red. Moments pointing into the plot are shown by ⊗, while moments pointing out of the plot are shown as ⊙. The intra-trilayer coupling as well as the coupling across stripes is labeled. (b) Three-dimensional perspective of the structure shown in (a).

three degrees of freedom: (i) direction of the spin axis, (ii) magnetic coupling between individual layers ("intra-trilayer" coupling), and (iii) magnetic coupling across charge stripes—the latter two of which are depicted in Fig. 3. As detailed in the Supplemental Material [34], models that fully explore these degrees of freedom have been investigated. Based on comparisons of the calculated $(hk0)$ maps and $(4/3, 0, l)$ cuts to the experimental observations, all models that did not possess antiferromagnetic coupling across the charge stripes, a spin axis with a significant component perpendicular to the charge stripes, and an antiferromagnetic intra-trilayer interaction could be eliminated. This intra-trilayer antiferromagnetic interaction can be understood by direct exchange between two d^9 ions each possessing a hole in its $d_{x^2-y^2}$ orbital [40,41] as has been argued for $YBa_2Cu_3O_{6+x}$ [42]. The model that best matches the data is shown in Fig. 3, and the resulting $(hk0)$ map and $(4/3, 0, l)$ cut are shown in Figs. 1(c) and 1(d), respectively. Although quantitative agreement between the calculated and measured intensities is impossible because of the unknown nuclear contribution to the cross-section, the model qualitatively reproduces the observed pattern in the $(hk0)$ plane, the width of the peaks in l, the observed maxima at $l = \pm 4$, and the weaker peak at $l = 0$. Comparisons between the calculations for $\vec{S}//\vec{b}$ and $\vec{S}//\vec{c}$ favor $\vec{S}//\vec{c}$ because of the relative distribution of intensities in the $(hk0)$ plane; specifically, as shown in the SI, the case of $\vec{S}//\vec{b}$ yields intensities that are too weak at $(1, 1/3, 0)$ and $(1, -1/3, 0)$.

Models of correlated trilayers have also been considered. We found that in these correlated models, the building units of individual trilayers must possess the same characteristics established for the uncorrelated trilayers discussed above: antiferromagnetic intra-trilayer interactions, antiferromagnetic coupling across charge stripes, and a spin axis perpendicular to the stripe direction. Significant broadening of the observed line shapes along l must be imposed to fit the data, yielding a correlation length along $\vec{c}$ that corresponds to roughly the height of a single trilayer. Thus, although weak coupling between nearest neighbor trilayers must be present, the data can be adequately modeled using a simplified uncorrelated trilayer model (intensities for correlated trilayer models are described in detail in the Supplemental Material [34]). Note that weak coupling along $\vec{c}$ is common in related materials such as LSNO [29]. In the case of $La_4Ni_3O_8$, this can be rationalized by the large distance between successive trilayers (~6.5 Å), the lack of a significant superexchange pathway connecting trilayers, the lateral shift in the Ni positions from one trilayer to the next (as shown in the Supplemental Material [34], Fig. 3) which leads to geometric frustration, and the short correlation length of charge stripes along $\vec{c}$ [13]. Moreover, layered structures such as $La_4Ni_3O_8$ often possess stacking faults with different numbers of layers that may also reduce the correlation between trilayer blocks.

An ordered moment pointing along $\vec{c}$ contrasts with the majority of quasi-2D cuprates, nickelates, manganites, and cobaltites for which the moment lies parallel to the ab plane. To understand this experimentally determined magnetic easy axis and to obtain the magnetocrystalline anisotropy energy, relativistic electronic structure calculations were performed (see the Supplemental Material for full details [34]). The results show that $\vec{c}$ is the spin axis, in agreement with the diffraction, with an anisotropy energy $\Delta E = E[010] - E[001] = 50\ \mu$eV/Ni. This value is consistent with the scale of anisotropy energy in cuprates [42]. The in-plane energy difference is smaller, $E[100] - E[010] = 2\ \mu$eV/Ni.

The temperature-dependent order parameter of the charge stripes, from the (13/3, 3, 0) superlattice reflection in x-ray measurements, is shown in Fig. 4(a). The magnetic order parameter [Fig. 4(b)] was measured as the temperature dependence of (4/3, 0, 4), which is suitable since the magnetic cross section peaks at $l = 4$, whereas the nuclear cross section does not. The magnetic order parameter was fit to a power law, $I \propto (1\text{-}T/T_N)^{2\beta}$, for $T < T_N$ (where T_N is the Néel temperature) with fixed β of 0.125, which corresponds to a 2D Ising system [43]. Inasmuch as the fit agrees reasonably well with the temperature dependence of the intensity, this suggests the order parameter is consistent with the quasi-2D Ising model described above. Direct determination of the exponent from free fitting would require a higher density of temperature points with significantly improved counting statistics compared to what could be measured. Within the temperature resolution of the measurements, both the charge and spin order

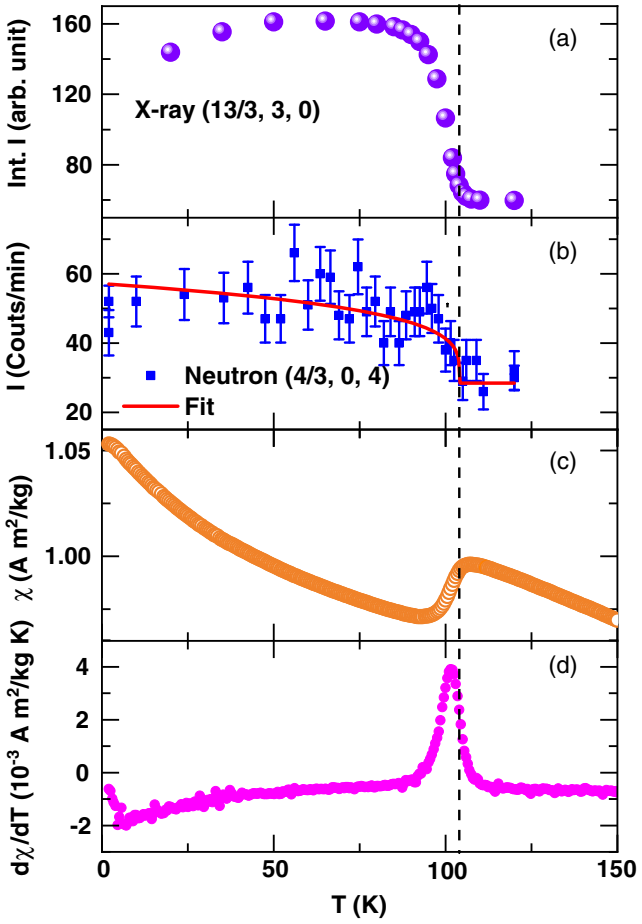

FIG. 4. Temperature dependence of the charge superlattice peak (13/3, 3, 0) measured with x rays (a), spin superlattice peak (4/3, 0, 4) measured with neutrons (b), magnetic susceptibility (c), and first derivative of the magnetic susceptibility (d). Uncertainties in (b) represent one standard deviation, derived from the square root of the number of counts. The fit in (b) corresponds to a power law as described in the text.

parameters become finite at the same temperature, consistent with the anomaly in the magnetic susceptibility [Fig. 4(c)]. In the single-layer nickelates, the lower spin-stripe transition temperature is manifest by a change in slope in the magnetic susceptibility [17]. Consistent with the spin and charge stripes possessing the same transition temperature in $La_4Ni_3O_8$, the slope of the susceptibility, shown in Fig. 4(d), evidences no such feature. We note a reduction in both order parameters at the lowest temperatures, the origin of which is not understood.

If one order were dominant, then its temperature dependence should be stronger than that of the secondary order parameter, which would go as the square of the primary order parameter. However, it is clear from Fig. 4 that both the charge and spin order parameters reach their maximum value at approximately the same temperature, suggesting a scenario of strongly coupled spin and charge stripes in which neither order parameter is secondary. This behavior contrasts with that of single-layer nickelates, as well as many other transition metal oxides, where the charge stripes order at a higher temperature than the spin stripes with the spin order having a temperature dependence consistent with its secondary nature [7]. Specific examples of other transition metal oxides that do exhibit simultaneous charge and spin stripe transitions include the three-dimensional perovskite $Nd_{1/3}Sr_{2/3}FeO_3$ [44], but which clearly has a dominant charge order parameter instead, as well as $Nd_{1/2}Sr_{1/2}MnO_3$ [45]. Thus, the simultaneous transitions in quasi-2D materials and nondominant order parameters appear particular to $La_4Ni_3O_8$.

Comparison of the correlation lengths in spin and charge channels may offer additional insights. Within the *ab* plane, both the charge and magnetic correlation lengths appear as long-range ordered, with the caveat that the quality of currently available crystals makes it impossible to differentiate correlation lengths larger than several nanometers from long-range order. Energy stability arguments based on the anisotropy energies indicate that the in-plane correlation length must be more than 2 nm. Along $\vec{c}$, the correlation length for both charge and spin is approximately the size of an individual trilayer. We do note, however, that correlation between nearest neighbor trilayers is required to reproduce the observed superlattice pattern in x rays [13], whereas such coupling is not necessary to reproduce the magnetic intensity observed here, though such coupling clearly cannot be ruled out.

In summary, neutron diffraction establishes an ordered magnetic ground state for $La_4Ni_3O_8$. The magnetic structure is an antiferromagnetic spin stripe state with spins commensurate with the charge stripes. The weak (3–4 orders of magnitude smaller than nuclear) and highly diffuse (along $\vec{c}^*$) magnetic reflections explain why no magnetic Bragg peaks have been reported in powder diffraction. This resolves a long-standing issue regarding the anomalous drop in magnetic susceptibility that occurs at ~105 K and corroborates ^{139}La nuclear magnetic resonance measurements that have been interpreted to reflect long-range antiferromagnetic order. Multi-domain stripes with weak or little inter-trilayer coupling may explain the broad distribution of hyperfine fields that were reported [20]. Our observations provide a unified spin stripe or charge stripe coupling picture in layered nickelates and complete the parallel between single-layer nickelates and trilayer nickelates. The square-planar nature of the trilayer material, combined with its *d*-electron count and large orbital polarization, make it appealing as a starting point for finding cupratelike superconductivity. Observation of antiferromagnetic spin stripes represents another intriguing parallel to cuprates, and suppression of the stripes via chemical substitution or electrolytic gating may represent means for achieving superconductivity. The intriguing question in the trilayer system is whether upon charge

carrier doping the physics will parallel the persistent stripe physics of single-layer nickelates or if superconductivity and related phenomenology will emerge as in the cuprates.

Work in the Materials Science Division at Argonne National Laboratory (crystal growth, characterization, neutron and x-ray scattering experiments, data analysis, and theoretical calculations) was supported by the U.S. Department of Energy, Office of Science, Basic Energy Sciences, Materials Science and Engineering Division. This research has been supported in part by ORNL Postdoctoral Development Fund by UT-Battelle, LLC under Contract No. DE-AC05-00OR22725 with the U.S. Department of Energy. This research used resources at the High Flux Isotope Reactor, a DOE Office of Science User Facility operated by the Oak Ridge National Laboratory. This work is based upon research conducted at the Cornell High Energy Synchrotron Source (CHESS) which is supported by the National Science Foundation under Grant No. DMR-1332208. Access to MACS was provided by the Center for High Resolution Neutron Scattering, a partnership between the National Institute of Standards and Technology and the National Science Foundation under Agreement No. DMR-1508249. The authors thank Shannon Watson for her assistance with the polarized ^{3}He cells on MACS.

[1] M. Hücker, M. V. Zimmermann, R. Klingeler, S. Kiele, J. Geck, S. N. Bakehe, J. Z. Zhang, J. P. Hill, A. Revcolevschi, D. J. Buttrey, B. Büchner, and J. M. Tranquada, Phys. Rev. B **74**, 085112 (2006).

[2] J. M. Tranquada, G. D. Gu, M. Hücker, Q. Jie, H. J. Kang, R. Klingeler, Q. Li, N. Tristan, J. S. Wen, G. Y. Xu, Z. J. Xu, J. Zhou, and M. V. Zimmermann, Phys. Rev. B **78**, 174529 (2008).

[3] M. Cwik, M. Benomar, T. Finger, Y. Sidis, D. Senff, M. Reuther, T. Lorenz, and M. Braden, Phys. Rev. Lett. **102**, 057201 (2009).

[4] A. T. Boothroyd, P. Babkevich, D. Prabhakaran, and P. G. Freeman, Nature (London) **471**, 341 (2011).

[5] Z. Sun, Q. Wang, A. V. Fedorov, H. Zheng, J. F. Mitchell, and D. S. Dessau, Proc. Natl. Acad. Sci. U.S.A. **108**, 11799 (2011).

[6] H. Ulbrich, D. Senff, P. Steffens, O. J. Schumann, Y. Sidis, P. Reutler, A. Revcolevschi, and M. Braden, Phys. Rev. Lett. **106**, 157201 (2011).

[7] H. Ulbrich and M. Braden, Physica (Amsterdam) **481C**, 31 (2012).

[8] J. M. Tranquada, AIP Conf. Proc. **1550**, 114 (2013).

[9] J. M. Tranquada, B. J. Sternlieb, J. D. Axe, Y. Nakamura, and S. Uchida, Nature (London) **375**, 561 (1995).

[10] M. R. Norman, Rep. Prog. Phys. **79**, 074502 (2016).

[11] V. V. Poltavets, K. A. Lokshin, A. H. Nevidomskyy, M. Croft, T. A. Tyson, J. Hadermann, G. Van Tendeloo, T. Egami, G. Kotliar, N. ApRoberts-Warren, A. P. Dioguardi, N. J. Curro, and M. Greenblatt, Phys. Rev. Lett. **104**, 206403 (2010).

[12] J. Zhang, A. S. Botana, J. W. Freeland, D. Phelan, H. Zheng, V. Pardo, M. R. Norman, and J. F. Mitchell, Nat. Phys. **13**, 864 (2017).

[13] J. Zhang, Y. S. Chen, D. Phelan, H. Zheng, M. R. Norman, and J. F. Mitchell, Proc. Natl. Acad. Sci. U.S.A. **113**, 8945 (2016).

[14] M. Greenblatt, Curr. Opin. Solid State Mater. Sci. **2**, 174 (1997).

[15] B. Keimer, S. A. Kivelson, M. R. Norman, S. Uchida, and J. Zaanen, Nature (London) **518**, 179 (2015).

[16] P. Kuiper, J. van Elp, D. E. Rice, D. J. Buttrey, H. J. Lin, and C. T. Chen, Phys. Rev. B **57**, 1552 (1998).

[17] R. Klingeler, B. Büchner, S. W. Cheong, and M. Hücker, Phys. Rev. B **72**, 104424 (2005).

[18] Z. Hu, M. S. Golden, J. Fink, G. Kaindl, S. A. Warda, D. Reinen, P. Mahadevan, and D. D. Sarma, Phys. Rev. B **61**, 3739 (2000).

[19] A. S. Disa, F. J. Walker, S. Ismail-Beigi, and C. H. Ahn, APL Mater. **3**, 062303 (2015).

[20] N. ApRoberts-Warren, A. P. Dioguardi, V. V. Poltavets, M. Greenblatt, P. Klavins, and N. J. Curro, Phys. Rev. B **83**, 014402 (2011).

[21] S. Sarkar, I. Dasgupta, M. Greenblatt, and T. Saha-Dasgupta, Phys. Rev. B **84**, 180411(R) (2011).

[22] J. G. Cheng, J. S. Zhou, J. B. Goodenough, H. D. Zhou, K. Matsubayashi, Y. Uwatoko, P. P. Kong, C. Q. Jin, W. G. Yang, and G. Y. Shen, Phys. Rev. Lett. **108**, 236403 (2012).

[23] T. Liu, G. Zhang, X. Zhang, T. Jia, Z. Zeng, and H. Q. Lin, J. Phys. Condens. Matter **24**, 405502 (2012).

[24] V. Pardo and W. E. Pickett, Phys. Rev. B **85**, 045111 (2012).

[25] W. Hua, New J. Phys. **15**, 023038 (2013).

[26] T. Liu, H. Wu, T. Jia, X. Zhang, Z. Zeng, H. Q. Lin, and X. G. Li, AIP Adv. **4**, 047132 (2014).

[27] A. S. Botana, V. Pardo, W. E. Pickett, and M. R. Norman, Phys. Rev. B **94**, 081105(R) (2016).

[28] V. Pardo and W. E. Pickett, Phys. Rev. Lett. **105**, 266402 (2010).

[29] S. H. Lee and S. W. Cheong, Phys. Rev. Lett. **79**, 2514 (1997).

[30] The commercial material, Cytop CTL-809m, is identified in this Letter to foster understanding. Such identification does not imply recommendation or endorsement by the National Institute of Standards and Technology.

[31] C. B. Fu, T. R. Gentile, G. L. Jones, W. C. Chen, R. Erwin, S. Watson, C. Broholm, J. A. Rodriguez-Rivera, and J. Scherschligt, Physica (Amsterdam) **406B**, 2419 (2011).

[32] Q. Ye, T. R. Gentile, J. Anderson, C. Broholm, W. C. Chen, Z. DeLand, R. W. Erwin, C. B. Fu, J. Fuller, A. Kirchhoff, J. A. Rodriguez-Rivera, V. Thampy, T. G. Walker, and S. Watson, Phys. Procedia **42**, 206 (2013).

[33] W. C. Chen, T. R. Gentile, Q. Ye, A. Kirchhoff, S. M. Watson, J. A. Rodriguez-Rivera, Y. Qiu, and C. Broholm, J. Phys. Conf. Ser. **746**, 012016 (2016).

[34] See Supplemental Material at http://link.aps.org/supplemental/10.1103/PhysRevLett.122.247201 for unit cell setting, additional polarized neutron scattering measurements, method of calculation of the magnetic intensity for uncorrelated trilayers, uncorrelated trilayer models for the spin ordering, models for the spin ordering that include

trilayer coupling, electronic structure calculations, and polarized data on MACS without efficiency correction, which includes Refs. [26,29,35–39].

[35] I. A. Zaliznyak and S.-H. Lee, Magnetic neutron scattering, in *Modern Techniques for Characterizing Magnetic Materials*, edited by Y. Zhu (Springer, Heidelberg, 2005).

[36] P. Blaha, K. Schwarz, G. K. H. Madsen, D. Kvasnicka, and J. Luitz, *WIEN2k: An Augmented Plane Wave Plus Local Orbitals Program for Calculating Crystal Properties*, (Vienna University of Technology, Austria, 2001).

[37] E. Sjöstedt, L. Nordström, and D. J. Singh, Solid State Commun. **114**, 15 (2000).

[38] J. P. Perdew, K. Burke, and M. Ernzerhof, Phys. Rev. Lett. **77**, 3865 (1996).

[39] D. J. Singh and L. Nordstorm, *Plane Waves, Pseudopotentials and LAPW Method* (Springer, New York, 2006).

[40] A. J. Freeman and R. E. Watson, Phys. Rev. **124**, 1439 (1961).

[41] C. Herring, in *Magnetism*, edited by G. T. Rado and H. Suhl (Academic Press, New York and London, 1966), Vol. IIB, p. 90.

[42] J. M. Tranquada, G. Shirane, B. Keimer, S. Shamoto, and M. Sato, Phys. Rev. B **40**, 4503 (1989).

[43] S. D. Wilson, C. R. Rotundu, Z. Yamani, P. N. Valdivia, B. Freelon, E. Bourret-Courchesne, and R. J. Birgeneau, Phys. Rev. B **81**, 014501 (2010).

[44] R. Kajimoto, Y. Oohara, M. Kubota, H. Yoshizawa, S. K. Park, Y. Taguchi, and Y. Tokura, J. Phys. Chem. Solids **62**, 321 (2001).

[45] P. W. Kolb, D. B. Romero, H. D. Drew, Y. Moritomo, A. B. Souchkov, and S. B. Ogale, Phys. Rev. B **70**, 224415 (2004).